Egyptian Journal of Radiology and Nuclear Medicine

RESEARCH

Open Access

Head and neck malignant lymphoma and squamous cell carcinoma discernment, is DWI conclusive?

Dina Gameel Anis[1], Maha Eshak Amer[1], Amany Saber Gerges[2], Moustafa Abdel Kader[3] and Sara Mahmoud Ragaee[3*]

Abstract

Background Differentiation between head-and-neck malignant lymphoma and squamous cell carcinoma is crucial as their management is radically different, and this retrospective study aims at demonstrating the value of DWI-MRI for their discrimination. Forty-four patients with pathologically proved untreated head-and-neck ML and SCC (22 ML and 22 SCC) were included in the study, and they underwent conventional MRI imaging (T1WI and T2WI) with DW-MRIs at standard and high *b*-values with corresponding ADC maps which were generated along with a reference of the ADC values taken at the spinal cord and cerebrospinal fluid as an internal control. The sensitivity and specificity at the optimum cutoff point as well as the area under the receiver operating characteristic (ROC) curve were used for evaluation of diagnostic performance of DW-MRI at *b* 1000, *b* 1500, *b* 2000 s/mm^2.

Results The mean SCC ADC values were much higher than ML at standard (*b* 1000) and high *b*-values (*b* 1500 and *b* 2000). ROC curve analysis for the ADC values of SCC and ML at *b* 1000, *b* 1500 and *b* 2000 s/mm^2 showed that the ADC cutoff values are >0.83, >0.75 and $>0.67\times10^{-3}$ mm^2/s, respectively, with diagnostic accuracy 95.5%.

Conclusions As to sum up, we can safely say that we can fully rely on DWI MRI in differentiation between HNSCC and ML whether using standard or high *b*-values, as well as in discrimination of different histological grades of HNSCC as it revealed impressive results, which confer us to do without contrast in such cases.

Keywords head-and-neck squamous cell carcinoma, HNSCC, Malignant lymphoma, ML, head-and-neck DW-MRI

Background

Head-and-neck region comprises variable tumors. Squamous cell carcinoma (SCC) is the most frequent malignant mucosal neoplasm that affects the head-and-neck. It accounts for over 90% of all malignant neoplasms [1], followed by malignant lymphomas (ML) which are second most common malignant tumor of the head-and-neck following SCC [2].

The management is radically different for these two different groups of malignancies. ML is treated by adjuvant therapy (chemotherapy, radiotherapy or a combination of both). However, SCC is best treated by complete surgical removal. So, it is important to differentiate ML from SCC as soon as possible in the early stages of the disease [2, 3].

Magnetic resonance imaging (MRI) is effective for diagnosing tumors. In addition to defining tumor's site, it also can provide additional information about tumor size, extension, lymph nodes involvement and intracranial invasion. However, conventional MRI examination cannot be used alone for differentiation between SCC and

*Correspondence:
Sara Mahmoud Ragaee
dr.sararagae@gmail.com; Sara.Mahmoud@mu.edu.eg
[1] Oral and Maxillofacial Radiology Department, College of Medicine and Dentistry, Minya University, Minya, Egypt
[2] Minya University, Minya, Egypt
[3] University of Medicine, Minya University, Minya, Egypt

lymphoma, as conventional MR imaging (both T1WI and T2WI) may show similar signal characteristics for both [4, 5].

Something that is remarkable for the functional imaging techniques such as DWI-MRI—which is noninvasive—is that it offers information regarding biological and functional aspects of the tumor in addition to its size and location [6, 7].

Assessment of DWI can be carried out in two ways, qualitatively, by visual assessment of signal intensity, and quantitatively, by measurement of the apparent diffusion coefficient (ADC) which quantifies water proton motion, in biological tissues [8].

In recent years, with improvements in MR Imaging gradient technology, high *b*-value ($b > 1000$ s/mm^2) DWI was introduced compared with standard *b*-value (*b* 1000 s/mm^2) DWI [9].

Aim of the work

The aim of this study was to determine the reliability of standard and high b-value DW-MRI in differentiation of head-and-neck malignant lymphoma and squamous cell carcinoma as well as in discrimination of different histological types of squamous cell carcinoma.

Methods

Cohort selection

In this retrospective study, 44 patients were selected from the outpatient oncology clinics in El Minya University Hospital and El Minya Oncology Center, during the period from July 2018 to September 2022. Selected patients were chosen regarding the inclusion criteria of being recently diagnosed, yet untreated pathologically proved ML or SCC in the head-and-neck region (Table 1). And the ones excluded from the study are those with other malignancies type rather than SCC and ML, treated patients by adjuvant therapy (radiotherapy, chemotherapy or both) or recurrent cases (Fig. 1).

This study was approved by the Research Ethics Committee (REC) under number 305 in 2018, Faculty of Dentistry, Minia University. Written, informed consent was obtained for all participants.

The 44 selected cases included twenty two patients with SCC (12 males, 10 females and mean age 58.4 years) and twenty two others with ML (14 males, 8 females and mean age 52.5 years).

Patient history and clinical examination

Each patient has undergone clinical examination through extra- and intra-oral routes with detailed history taking (Table 2). Then, patients have undergone either tru-cut image guided biopsy ($n=24$, 54.5%), excisional ($n=12$, 27.3%) or endoscopic biopsy ($n=8$, 18.2%) with histopathological analysis and further classification of the pathologically proved SCC into well-differentiated, moderately differentiated and poorly differentiated carcinomas (Fig. 2).

Table 1 Variable sites of SCC and malignant lymphoma

Tumor site	Carcinoma ($n=22$)		Lymphoma ($n=22$)	
	N	%	*N*	%
Larynx	10	45.5	4	18.2
Thyroid gland	0	0	2	9.1
Hypopharynx	2	9.1	0	0
Lymph nodes	0	0	6	27.3
Nasopharynx	2	9.1	0	0
Oral cavity	6	27.3	0	0
Oropharynx	0	0	8	36.4
Parotid gland	2	9.1	0	0
Submandibular space	0	0	2	9.1

MRI sessions

All MR examinations were performed with a 1.5-T whole-body MR unit (Ingenia 1.5 Tesla, Philips, Netherland), using head-and-neck circular polarization array surface coils.

Before diffusion-weighted image, T1-weighted images (1800/15)—repetition time msec/echo time (TE) msec, with two signals acquired, and T2-weighted images fast spin-echo images (360/75)—repetition time msec/echo time (TE) msec, with two signals acquired, were obtained in the transverse and coronal planes, with acquisition matrix of 224×256, slice thickness 4.0 mm, gap 1 mm, field of view 27×27 cm, number of acquisitions NEX 2, pixel resolution 0.7×1.1×4.0 mm; T2WI: TR=4000–6800 ms, while TE=80–100 ms, matrix size 512×256, section thickness 4.0 mm, intersection gap 1 mm, field of view (FOV) 27×27 cm, number of acquisitions NEX 2, pixel resolution 0.7×1.1×4.0 mm) (Fig. 3).

Transverse and coronal images covering the lesions and areas of drainage from regional lymph nodes were obtained. Sagittal planes were acquired only when necessary as one or more pulses of T1- or T2-weighted sequences (Table 3).

Diffusion-weighted MR imaging was performed by using the multiple-section spin-echo single-shot echo-planar sequence in the transverse plane. In application of DWI, any cystic or calcified portions were avoided.

In this sequence, diffusion weighting was achieved by applying a pair of motion-probing gradients, one before and the other after the 180° radio-frequency pulse of the spin-echo T2-weighted sequence (Fig. 4).

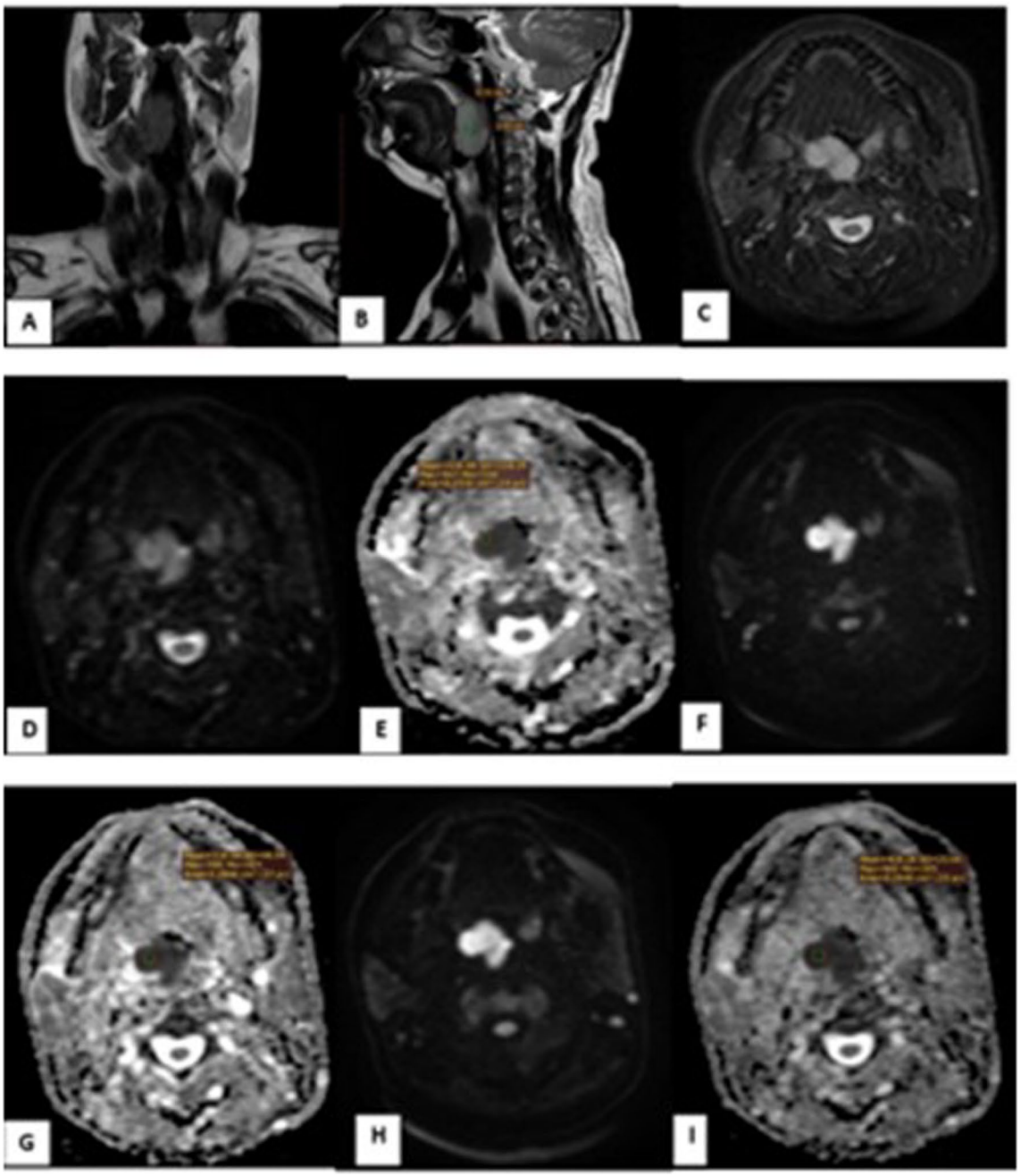

Fig. 1 Male patient, 65 years old, with pathologically proved oropharyngeal ML. **A** Coronal T1WI, **B** sagittal T2WI and **C** axial STIR, showing lobulated mass lesion (47 × 26 mm in dimensions) involving the right-sided supraglottic region, with inward bulging, significantly encroaching upon the air pathway rendering it narrowed. The lesion attains hypointense signal in T1WI with slightly hyperintense signal in T2WI and hyperintense fat suppression sequence. **D**, **E** DWI at $b = 1000$ s/mm^2 with corresponding ADC value of 0.63×10^{-3} mm^2/s. **F**, **G** DWI at $b = 1500$ s/mm^2 with corresponding ADC value of 0.53×10^{-3} mm^2/s. **H**, **I** DWI at $b = 2000$s/mm with corresponding ADC values of 0.42×10^{-3} mm^2/s. On DWIs, the lesion is seen truly restricted with increased brightness on elevation of the b-value from 1000 to 2000 s/mm^2

The single-shot echo-planar DW-MRI in the axial plane was obtained at different *b*-values—standard and high—(The standard *b*-value (*b* 0 and 1000 s/mm^2), where TR/TE were (2169 ms/73 ms), respectively, matrix size 192 × 182, section thickness 5. 0 mm, intersection gap 1 mm, field of view (FOV) 27 × 27 cm, pixel resolution (1.5 × 1.5 × 4.0) and the high *b*-values (*b* 0 and 1500 s/mm^2 and *b* 0 and 2000 s/mm^2), with TR/ TE (2464

Table 2 Comparison between ADC values (mm^2/s) in the two lesions, using repeated measures ANOVA test

b-value	Carcinoma ($n=22$)		Lymphoma ($n=22$)		*P* value (Between groups)	Effect size (Partial Eta Squared)
	Mean $\times 10^{-3}$	SD $\times 10^{-3}$	Mean $\times 10^{-3}$	SD $\times 10^{-3}$		
b 1000	1.03^{A}	0.2	0.67^{A}	0.09	< 0.001*	0.591
b 1500	0.95^{B}	0.17	0.61^{B}	0.09	< 0.001*	0.609
b 2000	0.86^{C}	0.16	0.56^{C}	0.08	< 0.001*	0.616
P value (Within group)	< 0.001*		< 0.001*			
Effect size (Partial Eta Squared)	0.796		0.649			

*Significant at $P \leq 0.05$; different superscripts in the same column are statistically significantly different

ms/81 ms) and (2698 ms/87 ms) respectively, matrix size 192×182, section thickness 4.0 mm, intersection gap 1 mm, field of view (FOV) 27×27 cm, pixel resolution (2×2 mm). The average scan time was 2 min 20 s for $b=1000$, 2 min 37 s for $b=1500$ and 2 min 52 s for $b=2000$ (Table 4).

All ADC maps were generated on the GE Medical Systems workstation. In order to generate the ADC maps, the signal intensity was calculated on DWI at the three different *b*-values (0 s/mm^2 and 1000 s/mm^2 for ADC map *b* 1000, 0 s/mm^2 and 1500 s/mm^2 for ADC map *b* 1500 and 0 s/mm^2 and 2000 s/mm^2 for ADC map *b* 2000) on a pixel-by-pixel basis.

Image analysis

Two reviewers (with 10 and 12 years of experience in interpreting head-and-neck MR images) were blinded to the histopathological results.

- The signal intensity (SI) of the lesions was evaluated in the conventional MR imaging (T1WI and T2WI) and was compared to the SI of surrounding muscles.
- The regions of interest (ROIs) were drawn manually by consensus on the ADC maps at *b* 1000 s/mm^2, with references of T1WI and T2WI, also as far as possible on the same region of approximately similar size (about 25–30 mm^2) on ADC maps of *b* 1500 s/mm^2 and *b* 2000 s/mm^2. The ROIs were drawn on a single slice in which the size of tumor was the largest. Three ROIs were measured of similar size from the solid portion of the mass to obtain a mean ADC value. Meticulous care was taken to avoid cystic, necrotic, hemorrhagic portion that might influence the ADC values and to avoid normal bony structures.
- The ADC values were compared in the HNSCC and the ML with further discrimination of the ADC values of SCC different histological grades as well.
- In order to evaluate the standardization and validity of our method, given the variety of localization and histopathological diagnosis of lesions (SCC and lymphoma), spinal cord and cerebrospinal fluid (CSF) ADC values were measured in the upper neck area and used as control values (Table 5).

Statistical analysis

Numerical data were explored for normality by checking the distribution of data and using tests of normality (Kolmogorov–Smirnov and Shapiro–Wilk tests). All data showed parametric (normal distribution). Parametric data were presented as mean and standard deviation (SD) values. For parametric data, Student's *t* test was used to compare between mean age values in the two groups. Comparison between ADC values of both groups as well as between variable *b*-value findings within each group was accomplished using repeated measures ANOVA test. Bonferroni's post hoc test was used for pair-wise comparisons. Frequencies and percentages were used to present qualitative data. Fisher's exact test was used to compare between the two groups. Construction of ROC (receiver operating characteristic) curve to determine the cutoff values for discrimination between SCC and ML, correlating them with the CSF and spinal cord ADC values as internal control. Areas under the ROC curve (AUCs) were compared using *z*-statistic. Statistical software version 19.5.1 was utilized for ROC curve analysis. The significance level was set at $P \leq 0.05$.

Results

- Regarding conventional MRI, there was no statistically significant difference in the findings and the signal intensity of HNSCC and malignant lymphoma between T1WI and T2WI with non-significant *P* value.
- Comparison between ADC values of carcinoma and lymphoma in all *b*-values

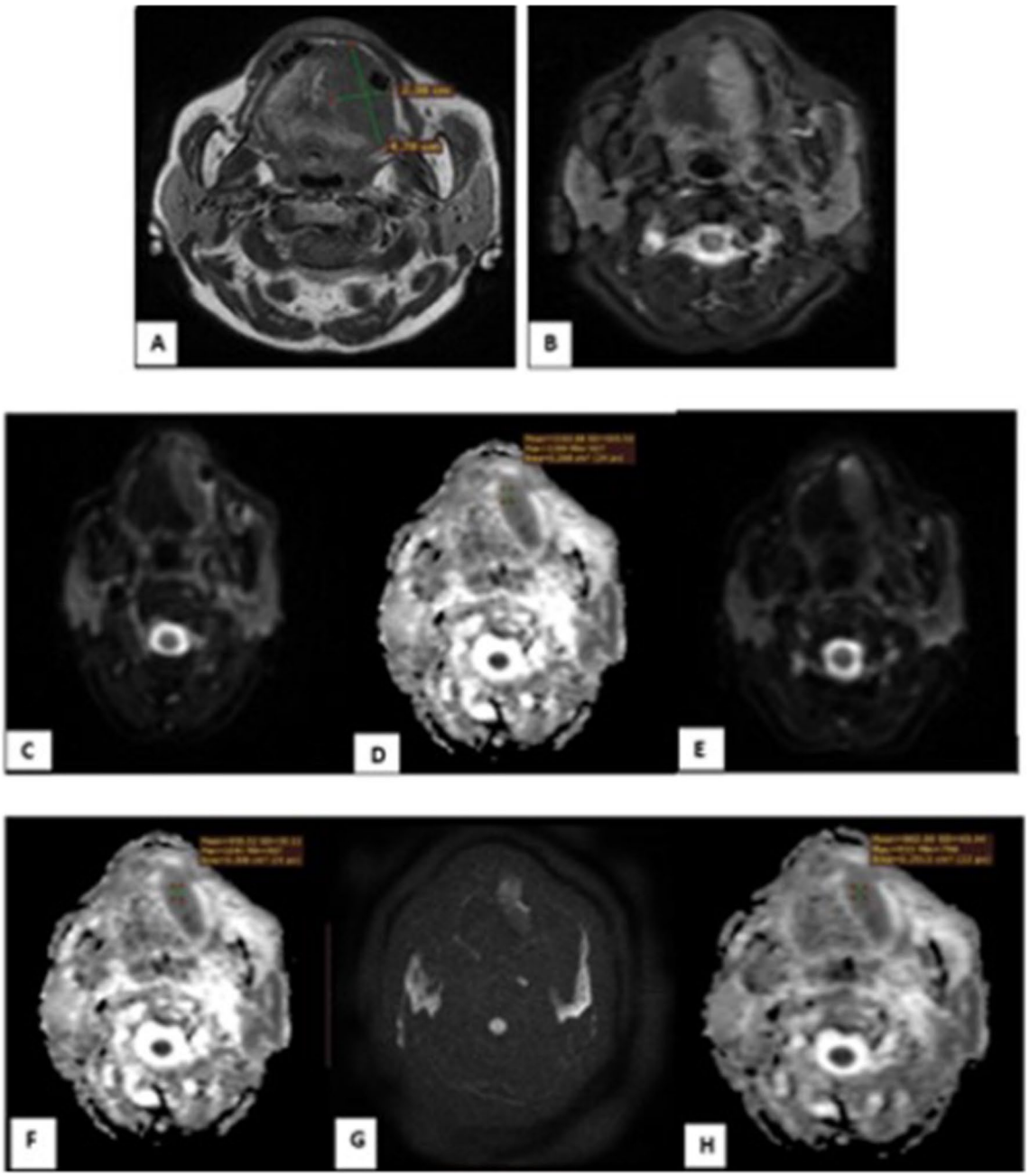

Fig. 2 Female patient, 45 years old, with pathologically proved tongue squamous cell carcinoma. **A**, **B** Axial T1WI and T2WI showing large ill-defined mass lesion (measuring 47 × 23 mm in dimensions) seen involving the left lateral aspect of the tongue, with no infiltration of the surrounding fat planes, respecting the tongue's borders. The lesion attains hypointense signal in T1WI with heterogeneous high signal in T2WI. **C**, **D** DWI at $b = 1000$ s/mm^2 with corresponding ADC value of 1.10×10^{-3} mm^2/s. **F**, **G** DWI at $b = 1500$ s/mm^2 with corresponding ADC value of 0.95×10^{-3} mm^2/s. **H**, **I** DWI at $b = 2000$s/mm with corresponding ADC values of 0.86×10^{-3} mm^2/s. On DWIs, the lesion is seen truly restricted with increased brightness on elevation of the *b*-value from 1000 to 2000 s/mm^2

- Carcinoma group showed statistically significantly higher mean ADC values than lymphoma group in all the used b-values (whether using *b* 1000, *b* 1500 or *b* 2000s/mm^2).
    - Pair-wise comparisons for the ADC values in the different b-values within each group revealed that the mean ADC value was disproportionate to the *b*-value, i.e., *b* 1000 s/mm^2 showed the sta-

tistically significantly highest mean ADC, while the b 1500 s/mm^2 showed statistically significantly lower mean ADC value and *b* 2000 s/mm^2 showed the statistically significantly lowest mean ADC value.

- o ROC curve analysis for ADC values of *b* 1000, *b* 1500 and *b* 2000s/mm^2 for discrimination between carcinoma and lymphoma showed that the cutoff ADC values are > 0.83, > 0.75 and > 0.67×10^{-3}mm^2/s, respectively (with the higher ADC values happened to be with carcinoma), with 95.5% diagnostic accuracy, a sensitivity of 90.9%, specificity of 100%, positive predictive value of 100% and negative predictive value of 91.7%.
- o No statistically significant difference was noted between the measures areas under the ROC curve (AUC) of the different *b*-values using the pair-wise comparison, as follows: *B* 1000 and *b* 1500 ($z = 0.606$, *P* value = 0.545), *b* 1000 and *b* 2000 ($z = 0$, *P* value = 1), *b* 1500 and *b* 2000 (z = 0.439, *P* value = 0.661).

- Comparison between ADC values of carcinoma grades and lymphoma
  - o With different b-values used in our study, well-differentiated SCC showed the highest mean ADC, and both moderately and poorly differentiated SCC showed lower ADC values, while lymphoma showed the lowest ADC value as shown in table [5].
- Comparison between ADC values of carcinoma, lymphoma and surrounding tissue as internal control
  - o In carcinoma group, there was a statistically significant difference between the measured ADC values in carcinoma and in CSF of upper neck at all *b*-values in our study. Pair-wise comparisons revealed that the CSF showed the statistically significantly highest mean ADC values. There was no statistically significant difference between the measured ADC values in carcinoma and spinal cord values; both showed statistically significantly lower ADC values than that of the CSF.
  - o As for lymphoma group, there was a statistically significant difference between the measured ADC values in lymphoma and in CSF of upper neck at all b-values in our study. Pair-wise comparisons revealed that the mean ADC value was significantly highest in the CSF, while it was statistically of lower value in the spinal cord and it was statistically significantly lowest in lymphoma.

Discussion

Squamous cell carcinoma (SCC) is the most frequent malignant mucosal neoplasm that affects the head-and-neck [1] followed by the malignant lymphomas (ML) [2]. The management is radically different for these two different groups of malignancies. So, differentiation of these two entities is crucial in the early stages of the disease [2, 3].

In the current study, we figured out that there was no statistically significant difference between SCC and ML groups in T1WI and T2WI (in conventional imaging) which is equivalent to the study conducted by Tomoko et al. [10] who showed that on both T1WI and T2WI, the signal intensities were not specific for ML or SCC.

Advanced MR imaging techniques as diffusion-weighted imaging (DWI) provide information regarding the molecular and pathophysiological aspects of a tumor. So, it can determine any microscopic pathologic alterations before they became visible on conventional MRI sequences [11].

High *b*-values (1000, 1500 and 2000 s/mm^2) were utilized in this study; therefore, the influence of perfusion was generally excluded, allowing the ADC values to approximate the true diffusion, thereby reflecting the cellularity, which is in rapprochement to the study conducted by Lu et al. [12] who inferred that the motion in biological tissues includes the molecular diffusion of water (true diffusion) and the microcirculation of blood (perfusion). At low *b*-values lower than 300 s/mm^2, the ADC would be limited because they were influenced by tissue perfusion.

ADC values were generated from DWI of standard *b*-value (*b* 1000) in this study. Of interest, we came out with the result that HNSCC showed statistically significant higher mean ADC value ($1.03 \pm 0.20 \times 10^{-3}$ mm^2/s) than lymphoma ($0.67 \pm 0.09 \times 10^{-3}$ mm^2/s). That was

(See figure on next page.)

Fig. 3 A male patient, 73 years old, suffering from change in quality of voice and dysphagia (proved pathologically as laryngeal SCC). **A**, **B** Axial T1- and T2-weighted image showing an abnormal signal intensity mass lesion (18 × 11 mm in size) involving the right glottis and supraglottic regions. The lesion displays iso- to hypo-signal in T1WI and hyperintense signal in T2WI. **C**, **D** DW-MRI at $b = 1000$ s/mm^2, the ADC map (mean ADC = 1.3×10^{-3} mm^2/s). **E**, **F** DW-MRI at $b = 1500$ s/mm^2, the ADC map (mean ADC = 1.2×10^{-3} mm^2/s). **G**, **H** DW-MRI at $b = 2000$ s/mm^2, the ADC map (mean ADC = 1.1×10^{-3} mm^2/s). The lesion is seen truly restricted on DWIs with low ADC values on the corresponding ADC maps with the lowest ADC value at $b = 2000$ s/mm^2

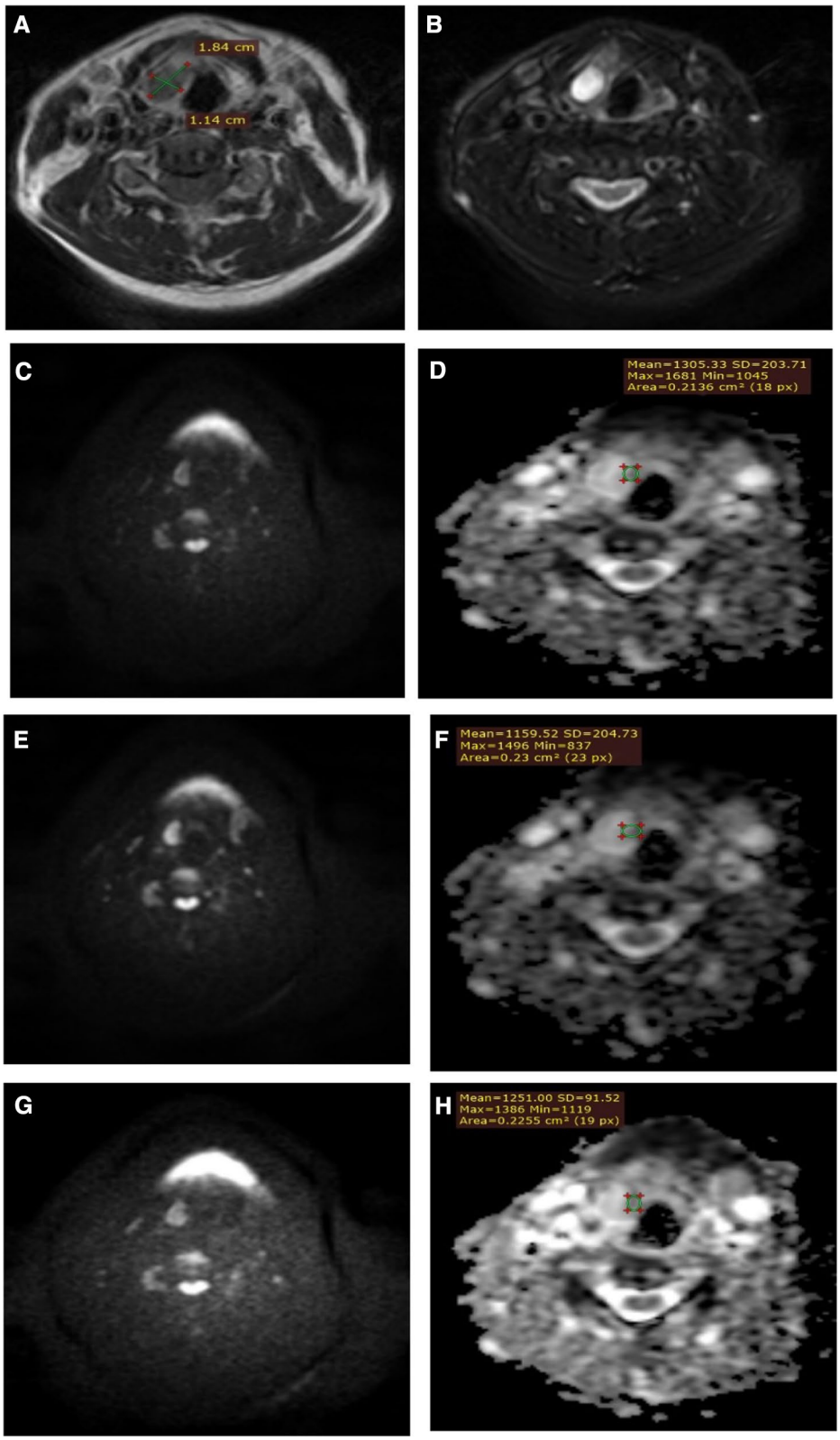

Fig. 3 (See legend on previous page.)

Table 3 Comparison between ADC values (mm^2/s) in carcinoma group and in normal values, using repeated measures ANOVA test

b-value	Carcinoma (*n* = 22)		Normal CSF (*n* = 22)		Normal spinal cord (*n* = 22)		*P* value	Effect size (Partial Eta Squared)
	Mean $\times 10^{-3}$	SD $\times 10^{-3}$	Mean $\times 10^{-3}$	SD $\times 10^{-3}$	Mean $\times 10^{-3}$	SD $\times 10^{-3}$		
b 1000	1.03^{B}	0.2	3.02^{A}	0.53	1.15^{B}	0.19	0.018*	0.444
b 1500	0.95^{B}	0.17	2.8^{A}	0.23	1.05^{B}	0.16	< 0.001*	0.985
b 2000	0.86^{B}	0.16	1.86^{A}	0.1	0.86^{B}	0.08	< 0.001*	0.978

*Significant at $P \leq 0.05$; different superscripts in the same row are statistically significantly different

close to what Tomoko et al. [10] reported in his study, where he stated that mean ADCs were smaller in lymphoma that SCC, using the high *b* factor of 1000 s/mm^2. In addition, Ichikawa et al. [13] mentioned that ADC-based differentiation between lymphomas ($0.503 \pm 0.099 \times 10^{-3}$ mm^2/s) and oropharyngeal carcinomas ($0.842 \pm 0.164 \times 10^{-3}$ mm^2/s) was possible. However, they reported that discrimination of nasopharyngeal carcinomas from lymphoma based on ADC values was not effective due to histological similarity of nasopharyngeal carcinomas and lymphomas.

We yielded significantly lower ADC values in malignant lymphoma than in HNSCC whether using *b* 1000, *b* 1500 or *b* 2000 s/mm^2, owing to the high cellularity in ML which acted as a diffusion barrier. So, the results of our study are consistent with the observation that the ADC is inversely associated with tumor cellularity, which is to a great extent similar to the study conducted by Pablo et al. [14] and Songtao et al. [15] who explained that the ADC values are substantially dependent on the changes in the diffusion of water protons from water to different tissue microstructures which depends on cell size, density, integrity of cellular membrane and tissue vascularity, so any changes in the tissue alter the ADC. Malignant lymphomas may have characteristically more cellularity, larger nuclei with more macromolecular proteins and less extracellular space than SCC.

It is worth mentioning that according to this study, ADC values have a substantial decrease by increasing the *b*-value over 1000 s/mm^2; as for the SCC and ML, the mean ADC values at b 1500 s/mm^2 decreased than at *b* 1000 s/mm^2, and the mean ADC values at *b* 2000 s/mm^2 decreased significantly than at *b* 1500 and *b* 1000 s/mm^2 that results are affirmed by the study conducted by DeLano et al. [16] who reported that the explanation of the negative correlation between the ADC values and the *b*-value could be that the apparent diffusion is more accurately represented by a biexponential relation. There would not be correlation if the relationship was monoexponential, where the ADC value should remain constant as the b-value increases.

Something to be considered in our study that the ROC curve analysis of ADC values in different b-values used in the study showed cutoff values of 0.83×10^{-3} mm^2/s, 0.75×10^{-3} mm^2/s and 0.67×10^{-3} mm^2/s, respectively, that in turn distinguish SCC from ML with sensitivity, specificity, PPV (positive predictive value), NPV (negative predictive value) and diagnostic accuracy of 90.9%, 100%, 100%, 91.7% and 95.5%, respectively. Likewise, the studies conducted by Tomoko et al. [10] and Vidiri et al. [17] where ADC thresholds in different *b* values were set of value 0.84×10^{-3} mm^2/s, 0.89×10^{-3} mm^2/s and 0.83×10^{-3} mm^2/s respectively to differentiate between these two lesions. That is quite different from the study conducted by Ichikawa et al. [13] where the ADC cutoff value at b factor = 1000 was 0.66×10^{-3} mm^2/s to discriminate oropharyngeal lymphomas from SCCs with higher sensitivity 100% and lower specificity 88%, 93% accuracy.

The current results inferred the ADC value of poorly differentiated (PD) SCC at different *b*-values, whether standard (*b* 1000) or high *b*-values (*b* 1500, *b* 2000) were lower than well-differentiated (WD) and moderately differentiated (MD) SCC. This agrees with Tomoko et al. [10] and Yun et al. [18] studies who stated that WD SCC had higher ADCs than poorly differentiated SCC at *b* 1000 and *b* 2000 s/mm^2. This can be explained by the

(See figure on next page.)

Fig. 4 A male patient, 52 years old, complaining of left sided neck swelling (proved pathologically as cervical lymphoma). **A**, **B** Axial T1- and T2-weighted image revealed multiple well-defined variable sized enlarged cervical lymph nodes (LNs) at the left side of the neck. The lesions appear isointense in T1WI and hyperintense signal in T2WI. **C**, **D** DW-MRI at $b = 1000$ s/mm^2, the ADC map (mean ADC value = 0.63×10^{-3} mm^2/s). **E**, **F** DW-MRI at $b = 1500$ s/mm^2, the ADC map (mean ADC value = 0.60×10^{-3} mm^2/s). **G**, **H** DW-MRI at $b = 2000$ s/mm^2, the ADC map (mean ADC value = 0.55×10^{-3} mm^2/s). The lesion is seen truly restricted on DWIs with notably low ADC values on the corresponding ADC maps with the lowest ADC value at $b = 2000$ s/mm^2

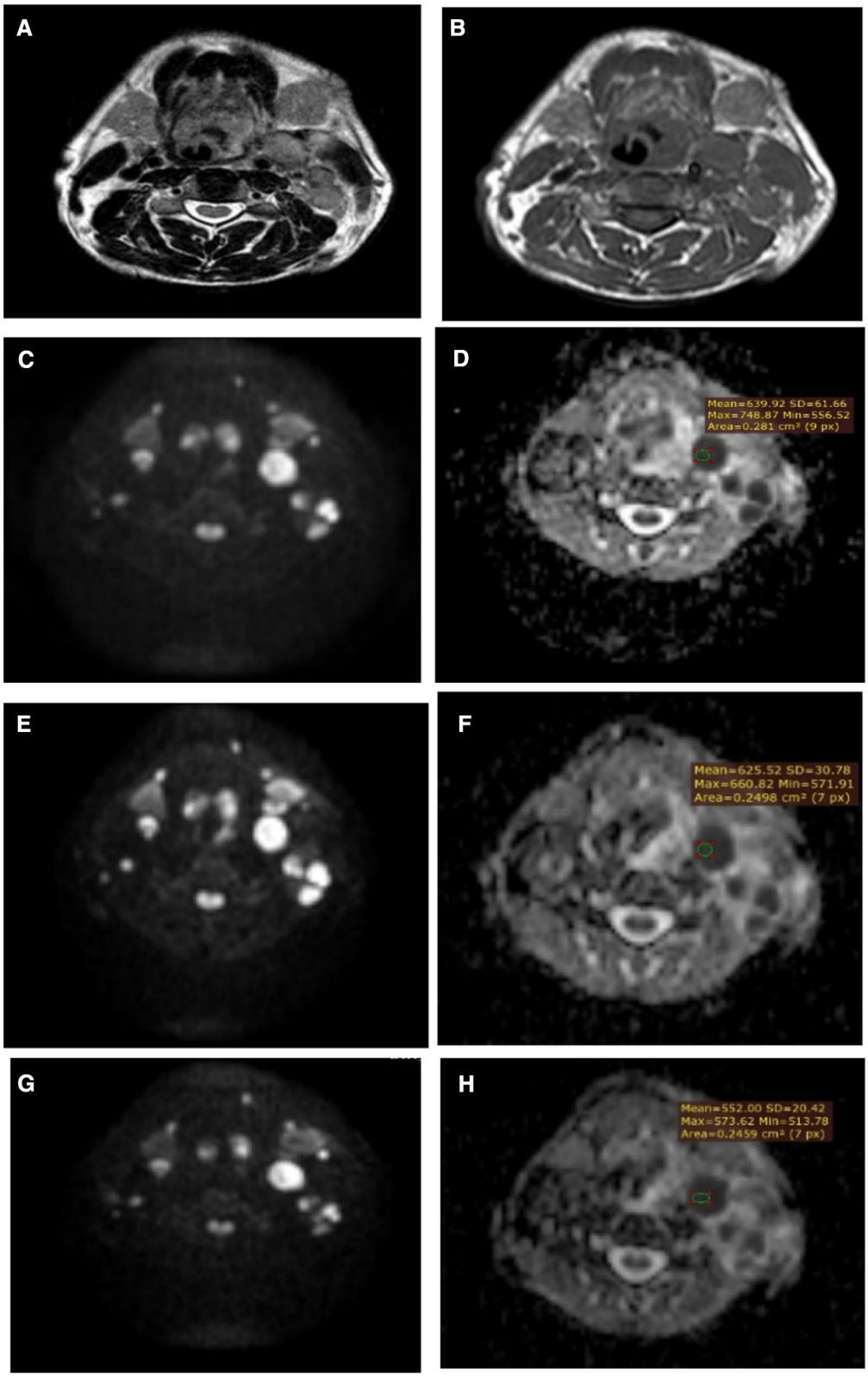

Fig. 4 (See legend on previous page.)

Table 4 Comparison between ADC values (mm^2/s) in lymphoma group and in normal values, using repeated measures ANOVA test

b-value	Lymphoma ($n=22$)		Normal CSF ($n=22$)		Normal spinal cord ($n=22$)		*P* value	Effect size (Partial Eta Squared)
	Mean $\times 10^{-3}$	SD $\times 10^{-3}$	Mean $\times 10^{-3}$	SD $\times 10^{-3}$	Mean $\times 10^{-3}$	SD $\times 10^{-3}$		
b 1000	0.67^{C}	0.09	2.86^{A}	0.42	1.09^{B}	0.11	< 0.001*	0.972
b 1500	0.61^{C}	0.09	2.26^{A}	0.22	0.91^{B}	0.1	< 0.001*	0.989
b 2000	0.56^{C}	0.08	1.87^{A}	0.14	0.77^{B}	0.08	< 0.001*	0.989

*Significant at $P \leq 0.05$; different superscripts in the same row are statistically significantly different

Table 5 Comparison between ADC values in carcinoma grades and lymphoma cases, using one-way ANOVA test

b-value	Well-differentiated SCC ($n=10$)		Moderately differentiated SCC ($n=6$)		Poorly differentiated SCC ($n=6$)		Lymphoma ($n=22$)		*P* value	Effect size (Eta Squared)
	Mean $\times 10^{-3}$	SD $\times 10^{-3}$	Mean $\times 10^{-3}$	SD $\times 10^{-3}$	Mean $\times 10^{-3}$	SD $\times 10^{-3}$	Mean $\times 10^{-3}$	SD $\times 10^{-3}$		
b 1000	1.2^{A}	0.14	0.97^{B}	0.11	0.82^{BC}	0.08	0.67^{C}	0.09	< 0.001*	0.83
b 1500	1.09^{A}	0.09	0.91^{B}	0.13	0.74^{BC}	0.05	0.61^{C}	0.09	< 0.001*	0.843
b 2000	0.98^{A}	0.07	0.86^{A}	0.13	0.66^{B}	0.04	0.56^{B}	0.08	< 0.001*	0.849

*Significant at $P \leq 0.05$; different superscripts in the same row are statistically significantly different

study of Bhatt et al. [19] who suggested that well-differentiated tumors are characterized by less mitotic activity resulting in low nucleus–cytoplasmic ratio, bigger size of cells and relatively low cellularity as compared to poorly differentiated high-grade malignancies. The degree of restricted diffusion would be higher for high-grade poorly differentiated tumors than low-grade well-differentiated malignant lesions.

Significant differences between the measured ADC values in HNSCC and normal CSF were observed in the current study, but not between HNSCC and spinal cord at both standard (*b* 1000 s/mm^2) and high *b*-values (*b* 1500 and *b* 2000 s/mm^2). That is in agreement with YUN et al. [18] who showed that there were significant differences between measured ADC values of HNSCC and CSF at both *b* 1000 and *b* 2000 s/mm^2. Also, the study conducted by Serifoglu et al. [20] greatly matches the current study in that at standard b-value there was no significant difference between HNSCC and spinal cord ADC values.

We also figured out that the ADC values measured in lymphoma, CSF and spinal cord showed statistically significant difference in different b-values. The highest mean ADC value was in CSF, followed by the spinal cord which was lower than that of lymphoma which was with the lowest mean ADC values. This coincides with the study conducted by Şerifoglu et al. [20] who applied ADC values in lesions' characterization at b-value 0 and 1000 s/mm^2. He found out that the mean ADC values of spinal cord and CSF were higher than that of ML.

The limitation of this study is that the HNSCC and ML population were quite heterogeneous as we included patients of various ages, with involvement of different neck regions and different pathological conditions which made the homogenization of our results difficult. Further studies with larger sample size might be needed to confirm findings of this study.

Conclusions

As to sum up, we can safely say that we can fully rely on DWI MRI in differentiation between HNSCC and ML whether using standard or high *b*-values, as well as in discrimination of different histological grades of HNSCC as it revealed impressive results, which confer us to do without contrast in such cases.

Abbreviations

HNSCC	head-and-neck squamous cell carcinoma
H&N	head-and-neck
ML	Malignant lymphoma
DWI	Diffusion-weighted imaging

Acknowledgements

The authors thank professors from Minya University Hospital for providing the software analysis tools and the technicians of the radiology department center. This work was supported by the Oral and maxillofacial Radiology Department of Minya university.

Author contributions

SMR and MAK carried out the manuscript preparation and editing, study concepts as well as the experimental studies and data analysis, design and

literature research, while ME is the Guarantor of integrity of the entire study and carried out the statistical analysis. DGA and AS were responsible for the clinical studies and also shared in the statistical analysis. All authors read and approved the final manuscript.

Funding
This research did not receive any specific grant from funding agencies in the public, commercial or not-for-profit sectors.

Availability of data and materials
The datasets used and analyzed during the study are available from the corresponding author upon reasonable request.

Declarations

Ethics approval and consent to participate
This study was approved by the Research Ethics Committee (REC) under number 305 in 2018, Faculty of Dentistry, Minia University. Written and informed consent was obtained for all participants.

Consent for publication
All patients included in this research gave written informed consent to publish the data contained within this study according to our institution rules for ethics committee.

Competing interests
The authors declare that there is no competing interests.

Received: 7 July 2023 Accepted: 30 September 2023
Published online: 11 December 2023

References

1. Thompson LDR (2003) Squamous cell carcinoma variants of the head and neck. Curr Diagn Pathol 9:384–396
2. Triantafillidou K, Dimitrakopoulos J, Iordanidis F, Gkagkalis A (2012) Extranodal non-hodgkin lymphomas of the oral cavity and maxillofacial region: a clinical study of 58 cases and review of the literature. J Oral Maxillofac Surg 70:2776–2785
3. El-Naggar AK, Chan JKC, Grandis JR, Takata T, Slootweg PJ (eds) (2017) Pathology and genetics of head and neck tumors: World Health Organization Classification of Tumors; 9(4)
4. Asaumi J, Yanagi Y, Konouchi H, Hisatomi M, Matsuzaki H, Kishiet K (2004) Application of dynamic contrast enhanced MRI to differentiate malignant lymphoma from squamous cell carcinoma in the head and neck. Oral Oncol 40:579–584
5. Grégorie V, Lefebvre JL, Licitra F, Felip E. EHNS-ESMO-ESTRO (2010) Guidelines Working Group. Squamous cell carcinoma of the head and neck: EHNS-ESMO-ESTRO Clinical practice guidelines for diagnosis, treatment and follow-up. Ann Oncol 21:184–6
6. Wang J, Shodayu T, Fumiyoshi T, Satoshi K, Akitoshi S, Tsuyoshi M, Mitsuhiro M, Tetsuya I (2001) Head and neck lesions: characterization with diffusion-weighted echo-planar MR imaging. Radiology 220:621–630
7. Thoeny HC (2007) Imaging of salivary gland tumors. Cancer Imaging 7:52–62
8. Koh DW, Collins DJ (2007) Diffusion-weighted MRI in the body: applications and challenges in oncology. AJR Am J Roentgenol 188(2):1622–1635
9. Seo HS, Chang KH, Na DG, Kwon BJ, Lee DH (2008) High *b*-value diffusion ($b = 3000$ s/mm^2) MR imaging in cerebral gliomas at 3T: visual and quantitative comparisons with $b = 1000$ s/mm^2. AJNRA 29(3):458–546
10. Tomoko S, Toru C, Daisuke I, Marie H, Chika H, Toyohiro K, Kunihiro M, Yuasa K (2016) MRI findings of extranodal malignant lymphoma and squamous cell carcinoma in the head and neck regions. Oral Radiol 32:98–104
11. Chawla S, Kim S, Wang S (2009) Diffusion-weighted imaging in head and neck cancers. Future Oncol 5(7):959–975
12. Lu Y, Jansen JF, Mazaheri Y, Stambuk HE, Koutcher JA, Shukla-Dave A (2012) Extension of the intravoxel incoherent motion model to non-gaussian diffusion in head and neck cancer. J Magn Reson Imaging 36:1088–1096
13. Ichikawa Y, Sumi M, Sasaki M, Nakamura T (2012) Efficacy of diffusion-weighted imaging for the differentiation between lymphomas and carcinomas of the nasopharynx and oropharynx: correlations of apparent diffusion coefficients and histologic features. AJNR Am J Neuroradiol 33:761–766
14. Pablo J, Inmaculada R, Teodoro M, Antonio Luna A (2013) Utility of MRI diffusion techniques in the evaluation of tumors of the head and neck. Cancers 5:875–889
15. Ai S, Zhu W, Liu Y, Wang P, Yu Q, Dai K (2013) Combined DCE and DW-MRI in the diagnosis of benign and malignant tumors of the tongue. Front Biosci 18:1098–1111
16. DeLano MC, Cooper TG, Siebert JE, Potchen MJ, Kuppusamy K (2000) High-b-value diffusion-weighted MR imaging of adult brain: image contrast and apparent diffusion coefficient map features. Am J Neuroradiol 21:1830–1836
17. Vidiri A, Silvia M, Francesca P, Raul P, Giovanni C, Ramy K, Giorgio C, Daniela R, Renato C, Simona M (2019) Cervical lymphadenopathy: can the histogram analysis of apparent diffusion coefficient help to differentiate between lymphoma and squamous cell carcinoma in patients with unknown clinical primary tumor? La Radiol Med 124:19–26
18. Yun TJ, Kim J-H, Kim KH, Sohn C-H, Park S-W (2013) Head and neck squamous cell carcinoma: differentiation of histologic grade with standard- and high-b-value diffusion-weighted MRI. Head Neck 35:626–631
19. Bhatt N, Gupta N, Soni N, Hooda K, Sapire JM, Kumar Y (2017) Role of diffusion-weighted imaging in head and neck lesions: pictorial review. Neuroradiol J 30(4):356–369
20. Serifoglu I, Ibrahim I, Murat D, Ozlem T, Omer Y, Zuhal E (2015) Diffusion-weighted imaging in the head and neck region: usefulness of apparent diffusion coefficient values for characterization of lesions. Diagn Interv Radiol 21:208–214

Publisher's Note